Journal of Pharmaceutical Sciences 112 (2023) 3022–3034

Contents lists available at ScienceDirect

Journal of Pharmaceutical Sciences

journal homepage: www.jpharmsci.org

Pharmaceutical Biotechnology

Solid-Solid Interfacial Contact of Tubing Walls Drives Therapeutic Protein Aggregation During Peristaltic Pumping

Thomas B. Fanthom[a], Christopher Wilson[b], David Gruber[b], Daniel G. Bracewell[a,*]

[a] Department of Biochemical Engineering, Bernard Katz Building, University College London, Gower Street, London, WC1E 6BT, UK
[b] Ipsen Biopharm, 9 Ash Road North, Wrexham Industrial Estate, Wales, LL13 9UF, UK

ARTICLE INFO

Article history:
Received 5 May 2023
Revised 13 August 2023
Accepted 13 August 2023
Available online 16 August 2023

Keywords:
Protein aggregation
Pumping
Peristaltic pump
Tubing
Interface
Contact
Stability
Antibody
Chromatography

ABSTRACT

Peristaltic pumping during bioprocessing can cause therapeutic protein loss and aggregation during use. Due to the complexity of this apparatus, root-cause mechanisms behind protein loss have been long sought. We have developed new methodologies isolating various peristaltic pump mechanisms to determine their effect on monomer loss. Closed-loops of peristaltic tubing were used to investigate the effects of peristaltic pump parameters on temperature and monomer loss, whilst two mechanism isolation methodologies are used to isolate occlusion and lateral expansion-relaxation of peristaltic tubing. Heat generated during peristaltic pumping can cause heat-induced monomer loss and the extent of heat gain is dependent on pump speed and tubing type. Peristaltic pump speed was inversely related to the rate of monomer loss whereby reducing speed 2.0-fold increased loss rates by 2.0- to 5.0-fold. Occlusion is a parameter that describes the amount of tubing compression during pumping. Varying this to start the contacting of inner tubing walls is a threshold that caused an immediate 20-30% additional monomer loss and turbidity increase. During occlusion, expansion-relaxation of solid-liquid interfaces and solid-solid interface contact of tubing walls can occur simultaneously. Using two mechanisms isolation methods, the latter mechanism was found to be most destructive and a function of solid-solid contact area, where increasing the contact area 2.0-fold increased monomer loss by 1.6-fold. We establish that a form of solid-solid contact mechanism whereby the contact solid interfaces disrupt adsorbed protein films is the root-cause behind monomer loss and protein aggregation during peristaltic pumping.

Introduction

Tangential flow filtration (TFF) is a ubiquitous unit operation in the manufacture of therapeutic proteins. It can be deployed in both upstream or downstream applications for perfusion culture[1,2] or ultrafiltration and diafiltration (UF/DF) operations, where, in these processes, solution is often recirculated for multiple hours using a pump to facilitate fluid transport.[3–5] Peristaltic pumping is a typical liquid handling solution employed in such settings as it is regarded as a low-shear solution to managing sensitive biologics. During UF/DF and peristaltic pumping, protein aggregation can occur.[4–9] Irreversible aggregation is the process of protein particle formation which leads to reduced manufacturing yields and can create complications in downstream processing such as membrane and resin fouling.[10,11] Controlling the amount therapeutic protein aggregation during bioprocessing is critical to maintaining critical quality attributes of drug products due to their known induction of immunogenic responses and potential to neutralise therapeutic efficacy.[12–14] Continuing to build our understanding of the possible protein aggregation mechanisms during bioprocessing is needed to build mitigation strategies during process development.

Protein aggregation can be caused by several different mechanisms that result in the unfolding of monomers to expose reactive sites for non-specific protein interactions.[15] Often, proteins adsorb onto interfaces existing at the boundaries of two phases, such as solid and liquid or air and liquid. These interfaces are found extensively throughout the manufacturing process and rates of aggregation are sensitive to materials in contact, local shear-stresses and liquid phase conditions. In pump apparatus, recent work has demonstrated that instantaneous shear stress is not a dependable indicator to define a pump's tendency to cause protein aggregation but are rather

Abbreviations: -ve BoNT/E, endopeptidase negative botulinum neurotoxin serotype-E; IICD, isothermal interfacial compression dilation cycle; mAb, monoclonal antibody; RPM, revolution per minute; SEC-UPLC, size-exclusion ultra-performance liquid chromatography; TFF, tangential flow filtration; UF/DF, ultrafiltration/diafiltration; UHMW-PE, ultra-high molecular weight polyethylene.

* Corresponding author.
E-mail address: d.bracewell@ucl.ac.uk (D.G. Bracewell).

https://doi.org/10.1016/j.xphs.2023.08.012

attributed to their fundamental mechanics.[16] In peristaltic pumping, rollers that compress on flexible tubing, to make a seal between the tubing walls and create pockets of liquid which the rotating motion of the pump head pushes through tubing to positively displace fluid. The measurement of compression applied to tubing is typically described as occlusion, defined in Eq. (1). At 100% occlusion, tubing inner walls contact as the rollers compress tubing. Peristaltic pumps can be fitted with fixed or variable occlusion beds to allow operators to vary this parameter depending on process requirements. However, these values are not often reported in literature or by manufactures.

Peristaltic pumping is thus complex, with a number of likely aggregation mechanisms such as: exposure heat generation from friction, adsorption to interfaces, fluidic shear stresses and foreign particles shed from tubing acting as nucleation sites.[8] The effect of heat produced during peristaltic pumping was investigated using thermal imaging on a peristaltic pump but the effect of pump parameters on heat gain were not tested and the internal temperatures of the pump head and tubing can be expected to be hotter than the outer pump body.[8] Tubing has been shown to affect the extent of particle production emanating from peristaltic tubing and protein aggregate formation.[6,7] However, particles shed from tubing have been shown to not affect aggregation rate of monoclonal antibodies (mAbs).[17] As mentioned, proteins can adsorb to interfaces where they can form protein films. Atomic force-microscopy has shown that this process is shorter than one second for silicone peristaltic tubing solid-liquid interfaces.[18] Once formed, expansion and relaxation of the solid-liquid interface during peristaltic pumping can cause protein film shedding and lead to the formation of protein particles.[8] This expansion mechanism is akin to isothermal interfacial compression dilation cycles (IIDCs) present in air-liquid interfaces.[19,20] In certain pumping systems, instances of cavitation can create air-liquid interfaces via bubble formation, however this does not seem to occur in peristaltic pumping.[8] A frequently suggested strategy to ameliorate protein loss is the addition of surfactants into protein formulations to inhibit protein adsorption, thus preventing aggregate formation.[6–8,18,21,22]

Contact- and friction-based protein film disruption mechanisms have been reported in previous literature: friction of interfaces is a known mechanism causing protein aggregation when a stirrer-bar interacts with a container surface during mixing[21], grinding of moving parts in a piston pump and a small-scale system that models contact causes protein aggregation[23] and, elsewhere in the milling of freeze-dried protein, grinding is another such mechanism that has been shown to cause covalent aggregate particle formation, although via the production of free radicals.[24] Based on these works, it could be expected that contacting of inner tubing walls could drive aggregation during peristaltic pumping, however investigation of such interface contacting mechanical-disruption mechanisms have not yet been systematically performed. [25–27]

In this work, we use one specifically built methodology to first investigate the effect of peristaltic pump parameters, pump speed and occlusion, on heat generation during pumping, and monomer loss and sample turbidity We further attempt to isolate potential underlining protein aggregation mechanisms and their effect on monomer loss by 1) utilising a methodology to quantity the impact of expansion-relaxation of solid-liquid interfaces (like one used by Deiringer et al.[25]) and 2) developing a novel methodology to quantify the impact of solid-solid interface contact in peristaltic tubing. In the former mechanism, elastomer tubing can expand and relax due to elasticity which could deform solid-liquid interfaces to cause protein aggregation like IICDs in air-liquid interfaces.[19,20]. This mechanism has been shown to cause varying amounts of protein particle formation depending on the type of peristaltic tubing used.[8,25] In the latter mechanism, peristaltic pumps operate by the occlusion of tubing which could lead to the contact of inner tubing walls, as we will refer to as solid-solid interface contact, which could cause protein aggregation similar to abrasion or grinding mechanisms previously described.[21,23,24]

During pumping studies, we use two-model therapeutic proteins: tocilizumab and endopeptidase negative botulinum neurotoxin serotype-E (-ve BoNT/E). These proteins are both ~150kDa and have an apparent melting temperature (T_m) of 45°C for -ve BoNT/E and 67°C for tocilizumab. A neutralised variant of serotype-E (-ve BoNT/E) is used which has a single mutation made in its primary structure that stops its cleaving function in a method described for botulinum neurotoxin serotype-A. [26] The two tested in tandem should complement each other in the goal of determining the root-cause aggregation mechanisms during peristaltic pumping.

Materials and Methods

Materials

We obtained stock solution of an endopeptidase negative (i.e. non-toxic) recombinant botulinum neurotoxin serotype-E, herein referred to as -ve BoNT/E, from Ipsen Biopharm. This stock solution is intermediate material having been purified partially following an initial chromatography step, hence there are host-cell proteins also present. We obtained a stock solution of tocilizumab from the Department of Biochemical Engineering (University College London, UK) having undergone purification using Protein A chromatography.

Both protein stock-solutions were reformulated using Slide-A-Lyzer® G2 2,500 MWCO PES 70mL dialysis cassettes purchased from Thermo Scientific (Rockford, IL, USA). Dialysis was conducted following manufacturer's instructions to exchange the protein stock solution buffer with 100mM sodium phosphate 100mM sodium chloride (pH 7.5) using a total dialysate buffer volume that is 200-times the sample volume used. This formulation is used throughout all experiments. All buffer components were acquired from Sigma-Aldrich Co. (St. Louis, MO, USA) and water obtained from a Milli-Q® Advantage A10 water system (Merck KGaA, Darmstadt, Germany). The total protein concentration was adjusted using Vivaspin® 20 3,000 MWCO PES centrifugal filters (Sartorius Stedim Lab Ltd, Stonehouse, UK), following manufacturer's instructions, to 0.4mg.ml^{-1} determined by a Nanodrop™ OneC Microvolume UV-Vis Spectrophotometer (Thermo Scientific) acquisition at 280nm. After formulation and concentration, solutions were filtered through a 0.22μm PVDF filter into 50mL falcon tubes and kept at 4°C prior to use. Protein solutions are filtered once again using a 13mm 0.22μm PVDF filter before their use in any studies.

Accelerated Protein Aggregation in a Closed-loop Pumping Method

A closed-loop device was built to accelerate the aggregation of tocilizumab and -ve BoNT/E during pumping (Fig. 1a). Two 160mm lengths of Masterflex® L/S® 15 High-Performance Precision Pump Tubing were joined together using two 3/16" Y-connectors. To provide an air-tight seal, and sample infusion and withdrawal during experiments, Luer-lock valves were joined to the ends of the Y-connectors with 1cm lengths of additional tubing. All tubing, Y-connectors and Luer locks were purchased form Cole Palmer Instruments Co. (Vernon Hills, IL, USA). The total volume of the built closed-loop device was 6.8mL. Pumping was facilitated using a Cole-Parmer Masterflex L/S® Console Drive 7521-40 (Cole Parmer Instruments Co.) with a Masterflex L/S® Easy-Load® II Pump Head with four rollers and a variable occlusion bed (Cole Parmer Instruments Co.) (Supplementary Fig. S1).

The closed-loop device was prepared prior to pumping by first wearing-in tubing by recirculating buffer solution at 40RPM for 10-minutes, then rinsing with MilliQ® water and leaving to dry. When

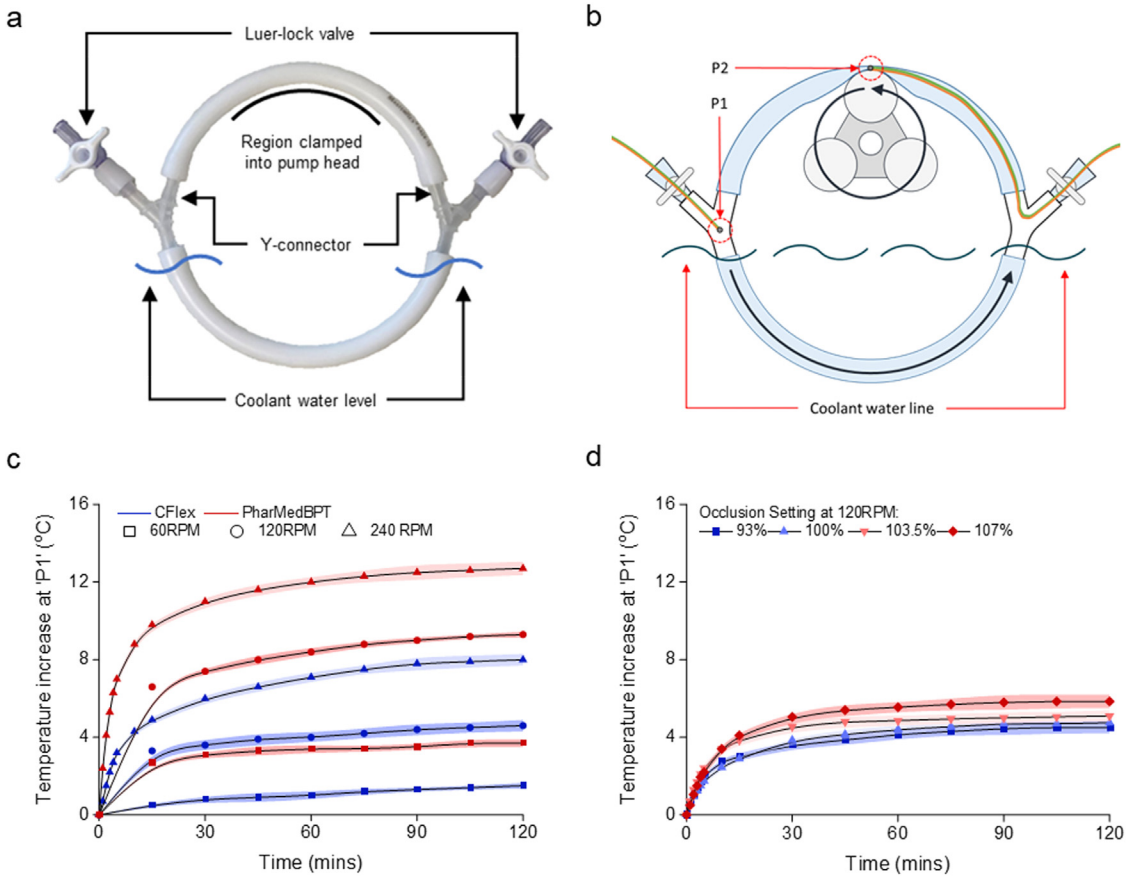

Figure 1. A closed-loop device demonstrates the effect of different peristaltic pump parameters on heat generation during pump operation and demonstrations that heat can cause aggregation of a therapeutic protein during pumping. **a** Illustration of the closed-loop device used for thermal studies during which it was filled with buffer solution formulated at 100mM sodium phosphate 100mM sodium chloride (pH7.5). **b** Locations of thermocouples inside the closed-loop device. **c** Temperature data captured by thermocouple at 'P1' and impact of pump speed on heat change in the buffer solution and differences caused by changing tubing type. Error bars represent the lower- and upper-limit of temperatures on the thermocouple readout and the points showing the median. **d** Temperature data captured by thermocouple at 'P1' and impact of occlusion on heat change in the buffer solution. Error bars represent the lower- and upper-limit of temperatures on the thermocouple readout and the points showing the median.

infusing the closed-loop with protein solution, it was rotated so that the Y-connectors are orientated vertically and perpendicular to the ground. Protein formulation was infused into the apparatus from bottom-up, thus pushing out all air and removing any air-liquid interfaces. The closed-loop device containing protein solution was allowed to incubate for five minutes prior to pumping.

Determining Temperature Change During Peristaltic Pumping Using a Closed-Loop Device

Temperatures inside the described closed-loop were monitored using two thermocouples positioned in two-separate locations (Fig. 1b). To read the buffer temperature, one thermocouple was positioned 60mm inside the tubing and upstream of the pump head by going through the Luer-lock. To read the tube surface temperature, a second thermocouple was positioned inside and centred within the occlusion zone by going through the remaining Luer-lock downstream of the pump head. The positions of these thermocouples are herein referred to as 'P1' (buffer zone) and 'P2' (occlusion zone) respectively. To seal Luer valve ends, a custom-shaped male-Luer end was used to fit around the thermocouple cables. The thermocouples used were K-Type, PFA insulated, flat-twin cables of diameter 0.3mm and welded ends. Pumping and temperature monitoring was conducted over two hours at varying pump speed (RPM) and occlusion (%) settings.

Determining Effect of Frictional Heat Gain on Monomer Loss During Peristaltic Pumping Using a Closed-Loop Device

The described closed-loop device was used with -ve BoNT/E solution, infused and formulated as described. -ve BoNT/E solution was recirculated in the closed loop device under the flowing conditions: 80RPM with no heat exchange, 80RPM with heat exchange to 20°C, 160RPM with no heat exchange and 160RPM with heat exchange to 20°C. Cooling was achieved by submerging half of the closed-loop device in cooled water provided by a Lauda Ecoline RE106 (LAUDA Technology Ltd, Stamford, UK) recirculating chiller set to a pre-calibrated temperature to maintain buffer temperatures of 20°C (Fig. 1b). Samples of protein solution were analysed using size-exclusion chromatography before and after experiments, which were conducted in duplicate.

Determining Effect of Peristaltic Pump Speed and Occlusion on Monomer Loss During Peristaltic Pumping Using a Closed-Loop Device

The closed-loop device was used to degrade tocilizumab and -ve BoNT/E under different rotational speed (RPM) and occlusion (%) settings to determine their effect on protein aggregation. During pump speed studies, rotational speeds (RPM) from 0RPM to 200RPM were used at increasing 40RPM intervals and maintaining constant 100% occlusion. During occlusion studies, occlusion settings of 93%, 96.5%, 100%, 103% and 107% were used at constant 80RPM speed. Occlusion is calculated using Eq. (1) where total tubing wall thickness is 't' and

distance between peristaltic rollers and occlusion bed is 'g'. All accelerated aggregation studies using the closed-loop device composed of Masterflex® L/S® 15 High-Performance Precision CFlex® tubing. Temperature of the protein solution was maintained at 20°C during pumping by removing the heat gain. This was done by submerging half of the closed-loop into cooled water provided by a recirculating chiller set to a pre-calibrated temperature. 100uL samples were withdrawn from the closed-loop every 15 minutes over two hours for size-exclusion chromatography analysis – therefore achieving a dilution of 1.5% per sample. These were retrieved by displacement through the infusion of an equivalent volume of buffer solution using a PhD Ultra programmable syringe pump from Harvard Instruments (Cambridge, MA). Experiments were run in duplicate.

$$Occlusion\ (\%) = \left(1 + \frac{2t - g}{2t}\right) * 100\% \quad (1)$$

Determining Effect of Expansion-Relaxation of Peristaltic Tubing Solid-Liquid Interfaces on Monomer Loss Using an Isolated Mechanism Method

A new device was developed to repeatedly strain tubing and determine what effect expansion and relaxation forces on peristaltic tubing solid-liquid interfaces has on protein aggregation. 50mm lengths Two Masterflex® L/S® 15 High-Performance Precision Pump peristaltic tubing variants, CFlex® and PharMedBPT®, were cut to be strained by using a PhD Ultra programmable syringe pump. Straining tubing was carried out by using syringe plungers, obtained from dismantled 5ml syringe (Thermo Scientific), with tubing over-locked on the plungers ends, to stretch tubing laterally outwards by a syringe pump.

To fill tubes, one tubing-end was initially fastened to a syringe plunger leaving the other end open allowing protein solution containing -ve BoNT/E to be added into the tube. Protein solution was degassed via vacuum prior to this to prevent air bubble formation during straining. The second plunger was pushed into the remaining open end of the tubing coming from a 45° angle to ensure no air was caught inside and removing any air-liquid interfaces. Joins between plungers and tubing were sealed tight using cable ties. Care was made to exclude all air. The syringe pump was programmed to repeatedly stretch them to 60mm (+20% strain) and relax, either 2,000- or 20,000-times, at a constant rate of 180cm.min^{-1}. Strain is defined by Eq. (2), where l_0 is the initial length and l is the strained length. Foil lined the actuating block and the top of the pump to reflective any radiating heat emanating from the syringe pump. Experiments were run in duplicate.

$$Strain,\ \% = \frac{l - l_0}{l_0} \quad (2)$$

Determining Effect of Solid-Solid Interfacial Contact in Peristaltic Tubing on Monomer Loss Using an Isolated Mechanism Method

An adaption of the closed-loop device was developed to create the device illustrated in Fig. 6a. Once assembled, the total hold-up volume was 6.8mL. The shorter 5.5cm piece of tubing was the segment that was occluded using a fabricated ultra-high-molecular-weight polyethylene (UHMW-PE) block of defined size, which itself was actuated upon using a programmable PhD Ultra syringe pump. Two ultra-high molecular weight polyethylene (UHMW-PE) blocks of sizes 10 × 10mm and 10 × 20mm were fabricated. giving contact areas of 0.48cm^2 and 0.96cm^2 (Fig. 7a).

-ve BoNT/E solution was infused carefully to remove all air and any air-liquid interfaces. Tubing was occluded 20,000-times within the ranges 0-35%, 50-85%, 60-95%, 65-100% and 70-105%. These ranges are selected to maintain a constant time variable and strain distances applied to tubing. Samples were withdrawn every 2,000-times by 100μL buffer displacement. Foil lined the actuating block and the top of the pump to reflective any radiating heat emanating from the syringe pump. Experiments were run in duplicate. A detailed methodology is within the supplementary material.

Size-Exclusion Ultra-Performance Liquid Chromatography (SEC-UPLC)

Analysis and quantification of -ve BoNT/E and tocilizumab monomer was conducted using an Agilent Technologies 1260 Infinity LC System (Santa Clara, CA) with degasser, binary pump, injector, temperature controller and diode-array detector (DAD). A Waters Corporation (Milford, MA) ACQUITY UPLC Protein BEH SEC 4.6 × 150mm 1.7um size-exclusion column and ACQUITY UPLC Protein BEH SEC Guard Column was equipped to the system. Analysis was conducted at 0.2ml.min^{-1} and 25°C with a 0.22μm filtered mobile phase formulated at 100mM L-Arginine 50mM sodium phosphate 100mM sodium chloride (pH 7.0). MilliQ® water was used in buffers and sourced from a Merck KGaA (Darmstadt, Germany) Advantage A10 water system. The column was first equilibrated with 5CVs of mobile phase before 10uL samples were injected. In accelerated protein aggregation studies using the peristaltic pump, sample preparation was conducted by filtering sample through a 4mm 0.22μm PVDF filter to remove spalled tubing particles and protein aggregates. Otherwise, samples were centrifuged at 18,000g for 10mins at 4°C. Proteins were quantified using a wavelength absorbance at 280nm with reference at 550nm. Where samples were recovered from studies using buffer displacement, the fractions of monomer quantities calculated using Eq. (2) where A_t is the integrated peak area at time t, A_0 is the integrated area at time 0 and 1.015 is the dilution factor (Eq. (3)).

$$Fraction\ of\ monomer\ remaining = \frac{A_t}{A_0} * 1.015 \quad (3)$$

Turbidity Measurements

Turbidity of degraded protein samples was analysed using a CLARIOstar® Plus plate reader from BMG LABTECH Ltd (Buckinghamshire, UK). 10μL of sample was loaded into a clear flat-bottom 384 well-plate, which subsequently briefly spun down in a centrifuge prior to analysis. Absorbance readings were taken at a wavelength of 350nm and blank data was taken from a time point of 0 minutes.

Results

Peristaltic Pump Parameters Can Affect Heat Generation During Pumping

The effect of pump speed on heat change during peristaltic pumping was investigated at 100% occlusion. Occlusion is the percentage of the total tubing wall thickness over the distance between the peristaltic roller compressing tubing and the peristaltic pump head wall where tubing is compressed against – at 100% occlusion, the total tubing wall thickness is equal to the distance between roller and pump wall, hence the tubing bore is closed and inner tubing walls begin to touch. After two-hours of pumping using CFlex® tubing, temperatures at 'P1' increased by 1.5±0.2°C at 60RPM, 4.6±0.3°C at 120RPM and 8.0±0.3°C at 240RPM (Fig. 1c). Changing the tubing to PharMedBPT® led to a further increase in temperature during pumping. The same pump speeds resulted in final temperature increases of 3.7±0.2°C at 60RPM, 9.3±0.2°C at 120RPM and 12.7±0.4°C at 240PRM after two-hours of pumping (Fig. 1c). Thus, swapping the peristaltic tubing to PharMedBPT® resulted in an average 2.0-fold increase in the heat generated compared to using CFlex® tubing.

We next investigated occlusion at a pump speed of 120RPM using CFlex® tubing (Fig. 1d). At 'P1' temperature change at 93% occlusion

(the distance between the roller and occlusion bed is 7% more than the total tubing thickness, thus under-occluding tubing) was +4.5±0.3°C and 100% occlusion was +4.8±0.2°C, indicating no change. However, increasing occlusion to 103.5% (the distance between the roller and occlusion bed is 3.5% less than the total tubing thickness, thus over-occluding tubing) and 107% resulted in an increase in temperature of +5.1±0.3°C and +5.9±0.4°C. It would be expected that above 100% occlusion setting, the increased friction and compression by contacting inner tubing walls would cause a sizeable increase in heat generation. To ensure that occlusion settings were accurate in regard to the point of inner tubing wall contact, they were calibrated against flow rates which demonstrated that fluid flow was established and steady from 100% occlusion (data not shown). Greater foreign tubing particle production at >100% occlusion also alluded to contact of interfaces creating spallation from the tubing wall in Supplementary Fig. S2.

When comparing temperature changes at 'P1' and 'P2' under 100% occlusion and using CFlex® tubing, the temperatures recorded at 'P2' were higher than at 'P1' at both pump speeds tested (Fig. 2a). Pumping at 80RPM the temperatures at 'P1' and 'P2' increased to 24.8°C and 28.8°C, respectively, whilst at 160RPM these were 27.3°C and 31.6°C. By these readings, temperatures recorded at position 'P2', corresponding to the surface temperature of the CFlex® tubing compressed by peristaltic rollers, were ~4.3°C higher than at 'P1'.

Heat Generation During Peristaltic Pumping is not a Dominant Protein Aggregation Mechanism

To determine if protein aggregation by thermal pathways play a dominant role in protein aggregation during pumping, the heat from during pumping was removed by heat exchange in a chilled water bath Cooling of the device was conducted by partially submerging in cooled water bath, as illustrated in Fig. 1a, which was calibrated to a set temperature to maintain 20°C. Thermal stability of -ve BoNT/E is considered to susceptible to aggregation at low temperatures - static light scattering of -ve BoNT/E during thermal ramping shows a low apparent melting point of ~38°C (Fig. 2b). Hence, it serves as an ideal model protein to use for such studies.

After pumping for two-hours at 80RPM, there was no notable difference in the monomer recovered when providing heat exchange and not. Upon increasing pump speed to 160RPM, providing heat exchange to cool the closed-loop apparatus resulted in improved monomer recovery of 6.7%. Whilst protein aggregation during peristaltic pumping can occur via thermal degradation, 89% of monomer is still lost due to other more dominant mechanisms yet to be determined. The sensitivity of -ve BoNT/E to heat during fast peristaltic pump speeds in the closed-loop device requires some heat exchange to cool the device down to 20°C and mitigate heat effects when investigating the mechanisms of protein aggregation using the closed-loop device. We calibrated pump speed against the coolant temperature required to maintain 20°C in the closed-loop device: 17.5°C at 40RPM, 16.4°C at 80RPM, 15.1°C at 120RPM and 13.8°C at 160RPM. In practice during UF/DF large volumes of working solution might have the heat capacity to remove excess heat during pumping removing the need for refrigeration.

Rate of Monomer Loss Per Peristaltic Roller Impact Has an Inverse Relationship to Pump Speed

The decay of tocilizumab and -ve BoNT/E monomer during pumping can be seen in SEC chromatograms in Fig. 3a. The presence of soluble low-molecular weight or high-molecular weight aggregate species were not observed in chromatograms, as is commonly reported in literature. The following monomer data is reported as a duplicate average. During control studies, conducted by incubating proteins within the closed-loop device for two-hours without pumping, 96.3% of tocilizumab and 94.7% of -ve BoNT/E monomer remained (Fig. 3b-c) – the losses here can be attributed to adsorption in the device and during handling of samples. After pumping

a

Pump Speed (RPM)	80		160	
Thermocouple location (-)	P1	P2	P1	P2
Temperature after two-hours pumping (°C)	24.8	28.8	27.3	31.6

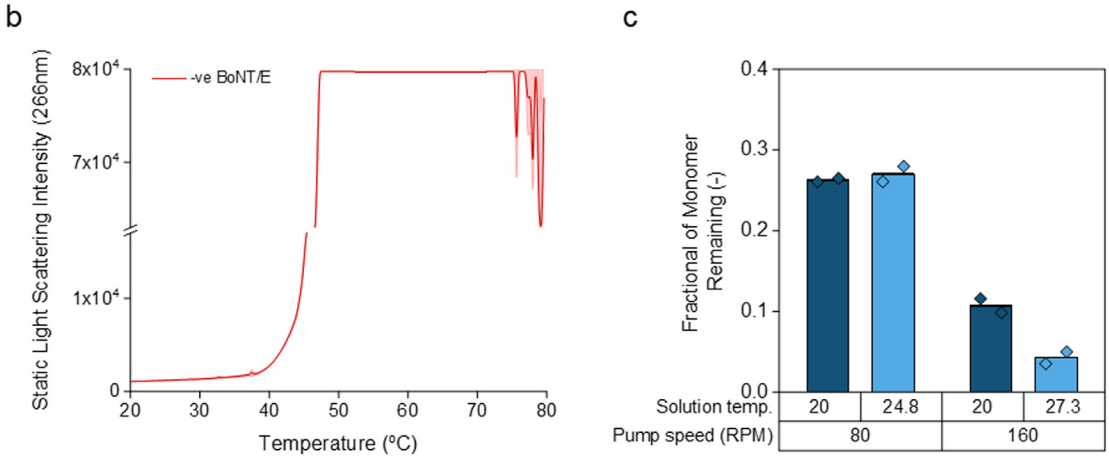

Figure 2. Heat generation in pumped buffer solution is the result of frictional forces of peristaltic rollers occluding tubing and that heat dissipating into the pumped solution. **a** Temperature differences between thermocouples at position 'P1' and 'P2' after two-hours of pumping at pump speed 80PRM and 160RPM. **b** Static light scattering conducted at 266nm of –ve BoNT/E formulated at 0.4mg/ml^{-1} 100mM sodium phosphate 100mM sodium chloride (pH7.5) during thermal ramping from 20°C to 80°C. **c** Fractions of remaining –ve BoNT/E monomer after conducting accelerated protein aggregation studies whilst pumping at 80RPM and 160RPM whilst allowing the solution inside the device to naturally heat up against cooling the device to an internal temperature of 20°C.

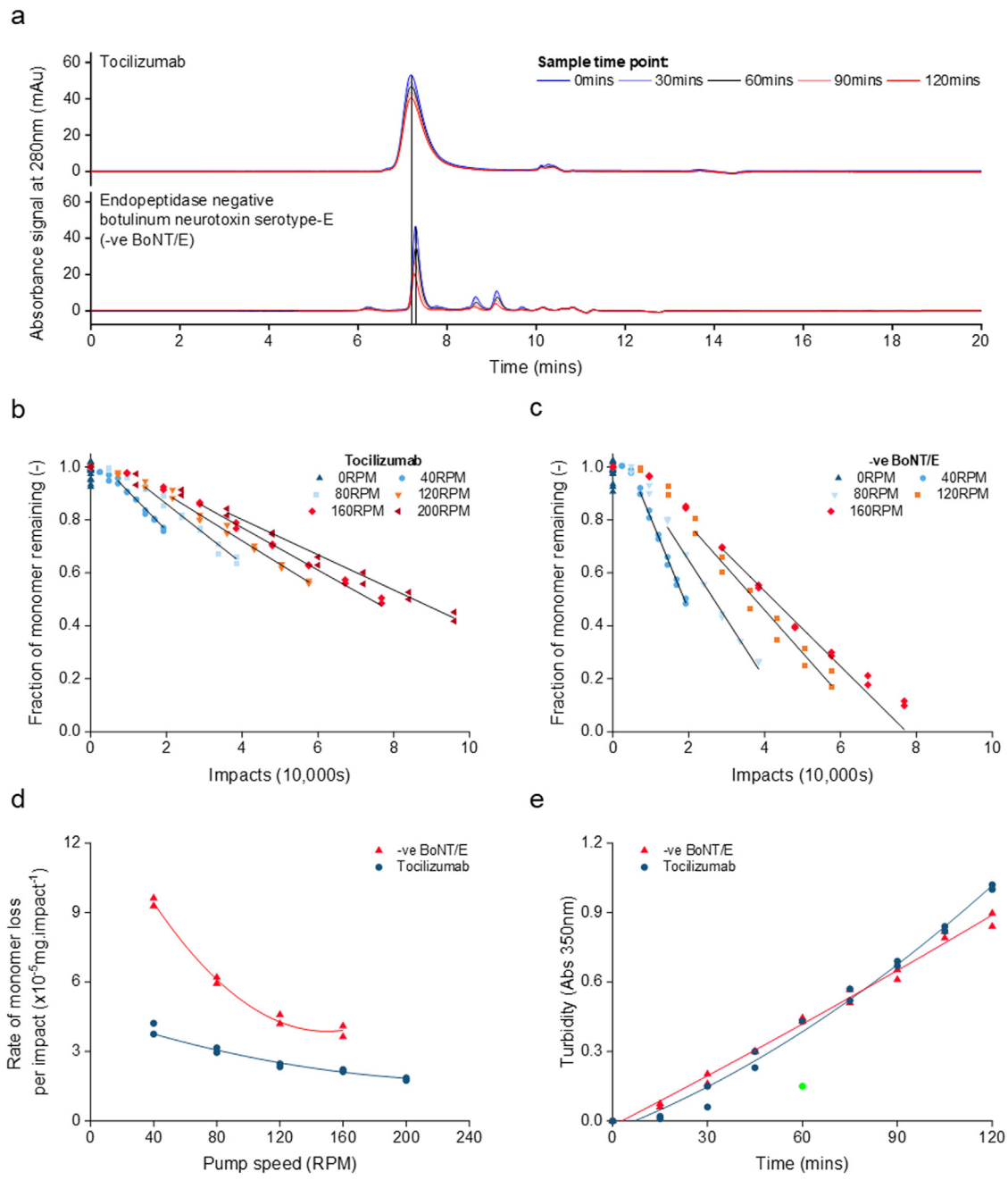

Figure 3. Monomer loss and protein aggregate formation occurring during peristaltic pumping acts in an inverse relationship to pump speed. **a** Chromatograms of two-model proteins, tocilizumab and −ve BoNT/E, both formulated at 0.4mg.ml^{-1} 100mM sodium phosphate 100mM sodium chloride (pH7.5), subjected to accelerated protein aggregation pumping studies and analysed using size-exclusion ultra-performance liquid chromatography. Samples were withdrawn from the closed-loop device at 15-minute intervals for analysis. **b-c** Fractions of remaining tocilizumab monomer **(b)** and −ve BoNT/E monomer **(c)** at different time points were correlated against the number of peristaltic roller impacts corresponding to each time-point. Linear regressions show concatenate fits to the duplicate data from the fourth-sample point correlate with an R^2 >0.99, other than -ve BoNT/E samples at 160RPM. **d** Maximum rates of tocilizumab and −ve BoNT/E monomer loss per impact (x10^{-5}mg.impact^{-1}) from the gradients of independent linear regressions of monomer loss data plotted in 'd' and 'c' are correlated against the corresponding pump speed (RPM). Second-order polynomial curves show concatenate fits to duplicate data with an R^2 >0.99. **e** Turbidity analysis was conducted on samples collected during pumping at 40RPM by absorbance at 350nm. Second-order polynomial curves show concatenate fits to duplicate data with R^2 0.99

tocilizumab for two-hours, percent monomer remaining was 76.4% at 40RPM, 64.6% at 80RPM, 56.5% at 120RPM, 49.5% at 160RPM and 43.4% at 200RPM (Fig. 3b). After pumping -ve BoNT/E for two-hours, percent monomer remaining at was 49.4% at 40RPM, 26.5% at 80RPM, 19.8% at 120RPM and 10.7% at 160RPM (Fig. 3c) – 200RPM was not conducted for -ve BoNT/E.

An interesting relationship was noticed. To cause 20% tocilizumab monomer loss at 40RPM, 18,000 pump head impacts were required. However for pump speeds of 80RPM, 120RPM, 160RPM and 200RPM an increasing 25,000, 32,000, 38,000 and 41,000 impacts were required (Fig. 3a). This trend is more significant the case of -ve BoNT/E (Fig. 3b). To better observe this relationship, the maximum rates of monomer loss per roller impact (x10^{-5}mg.impact^{-1}) were extracted from linear regressions on the monomer fractions correlated against occlusions (Fig. 3b and c). Due to a lag phase noticed within the first three samples of all monomer time-points, linearity was assumed

beyond the fourth sample time-point which gave R^2 values on average >0.99 across both model proteins.

An inverse relationship is evident between monomer loss per impact and pump speed, which follows an apparent second-order relationship (Fig. 3d) - a fitted parabola curve to the data has an R^2 of >0.99. For tocilizumab, the maximum rates of monomer loss per occlusion at 40RPM and 160RPM were 4.0×10^{-5}mg.impact^{-1} and 2.2×10^{-5}mg.impact^{-1} respectively (Fig. 3d). Whilst for -ve BoNT/E these rates at 40RPM and 160RPM were 9.5×10^{-5}mg.impact^{-1} and 3.9×10^{-5}mg.impact^{-1} (Fig. 3d). Thus, decreasing pump speed 4.0-fold resulted in a 1.8-fold increase in the rate of monomer loss for tocilizumab and 2.4-fold for -ve BoNT/E.

During visual inspection of samples, they appeared to turn progressively cloudy indicating potential formation of insoluble aggregates. We tested samples at 40RPM for turbidity changes using absorbance at 350nm (Fig. 3e) which showed an increase in absorbance over time for both tocilizumab and -ve BoNT/E which are indicative of the presence of insoluble protein aggregates.

The higher rates of -ve BoNT/E monomer loss compared to tocilizumab can be noted in Fig. 3d. Botulinum neurotoxins are known for having electric dipoles across their protein structure. These drive its reorientation for interaction with presynaptic membranes at a high rate and affinity.[27] Given that the peristaltic tubing is composed of a silicone rubber that is a negatively charged material, it is a possible explanation for the faster rates seen for -ve BoNT/E compared to tocilizumab.

Varying Occlusion Shows Key Protein Aggregation-Mechanism Changes as Inner Tubing Walls Begin to Contact

The pump apparatus, occlusion can be varied from 93% to 107%. When pumping for two-hours at 80RPM (40,000 rollers impacts) using the closed-loop device, we increased occlusion at intervals of 3.5% from 93%, following pre-set notches in the pump, to traverse the transition point of 100% where the inner tubing walls begin contacting. The following monomer data is reported as a duplicate average. For tocilizumab, monomer remaining was quantified at 69.3% at 93% occlusion, 66.0% at 96.5% occlusion and 64.5% at 100%, showing minor change in losses (Fig. 4a). Upon increasing occlusion settings above 100% to 103.5% and 107%, there was an immediate decrease in the fraction of monomer remaining to 46% and 24%, respectively. For -ve rBoNT/E, a similar trend and transition is seen. Monomer remaining was quantified at 68.7% at 93% occlusion and 57.5% at 96.5% occlusion, but suddenly decreased to 26.4% at 100% occlusion, 18.0% at 103.5% occlusion and 11.5% at 107% occlusion.

We analysed samples for changes in apparent turbidity shown in Fig. 4b and increasing absorbance for both proteins was acknowledged, which typically indicates increasing formation of insoluble protein aggregates with occlusion. Increasing occlusion can also trigger increased spallation from the tubing which may influence turbidity, so in a separate study, to see the effect of occlusion on foreign particle production via spallation, we pumped buffer solution under the same conditions. Here we saw an increasing presence of nanoparticles with occlusion as analysed by nanoparticle tracking analysis (Supplementary Data Fig. S2). This however led to negligible changes in turbidity (data not shown).

Expansion-Relaxation of Peristaltic Tubing Solid-Liquid Interfaces Play a Minor Role in Therapeutic Protein Monomer Loss

We developed a new method to repeatedly strain peristaltic pump tubing to recreate expansion-relaxation of peristaltic tubing outside of the pumping apparatus to determine if straining of the tubing is an important protein aggregation mechanism (Fig. 5a). In these studies, only one model protein, -ve BoNT/E, was used which in previous studies was the most prone to aggregation. The following monomer data is reported as a duplicate average.

After 2,000 expansion-relaxation cycles of CFlex® tubing by straining up to +20% of the tubing length, there was no difference in the monomer recovery of -ve BoNT/E in strained and non-strained tubing. Monomer remaining was quantified at 96.7% for the strained tubing and 96.9% for the non-strained tubing (Fig. 5b). When changing the tubing type to PharMedBPT®, applying 2,000 expansion-relaxation cycles, also caused no notable difference between strained and non-strained tubing - 96.6% and 97.1% monomer was quantified in the strained and non-strained PharMedBPT® tubing. For 20,000 cycles, low monomer recoveries obtained for all non-strained tubes may be due to heat emanating from the syringe pump during operation as the non-strained tubes are still positioned on top of the syringe pump during operation.

Increasing the total number of expansion-relaxation cycles to 20,000, there was no notable difference between monomer quantified from strained and non-strained CFlex® tubing. Monomer remaining was 94.4% and 94.0% for non-strained and strained CFlex® tubing. However, after straining PharMedBPT® 20,000 times, 2.3% more monomer was lost in the strained tubing compared to the non-strained tubing where 93.9% monomer remained.

Peristaltic Tubing Solid-Solid Interfacial Contact Can Cause Therapeutic Protein Monomer Loss

We developed a method (Fig. 6a) that is adapted from the closed-loop device (Fig. 1a) to isolate the effect of solid-solid interfacial linear-contact on monomer loss outside of a peristaltic pump. In SEC chromatograms of sample analysed after occluding tubing in the range 65-100%, -ve BoNT/E monomer peaks, eluting at 7.4 minutes, were seen to decrease with each time-point. As with earlier chromatograms, no soluble low-molecular weight or high-molecular aggregates were detected (Fig. 6b). Plotting fraction of monomer remaining against the time of sampling reveals trends which appear initially erratic (Fig. 6c). This may be due to low flow rates causing poor internal mixing of the buffer infused into the device. At the end of two-hours pumping, monomer loss data obtained at higher occlusion ranges diverges from lower ranges with trends becoming clearer (Fig. 6c). The following monomer data is reported as a duplicate average. In the control study, 96.0%. of -ve BoNT/E monomer remained. Upon occluding tubing, remaining monomer continuously decreases 96.0%, 94.7%, 93.7%, 88.6% and 89.7% at occlusion range upper-limit values of 35%, 85%, 95%, 100% and 105%.

Linear regressions were conducted on the monomer fractions correlated against the number of impacts to determine the rates of monomer loss per impact of the occlusion block (x10^{-5}mg.impact^{-1}) (Fig. 6c). Data was again assumed linear from the fourth sample time-point. Due to the noise of the data the R^2 values on average were 0.81. The rate of monomer loss per impact was obtained from the linear gradients were plotted against the upper limit of the respective occlusion ranges (Fig. 6d). The following monomer loss rates are reported on a duplicate average. At 0% occlusion, (control) protein solution was incubated in the device as a control study and resulted in an equivalent monomer loss rate of 1.01×10^{-5}mg.impact^{-1} – samples were taken at 40min intervals equal to 2000 impacts. Occluding tubing between 0-35% and 50-85%, rate losses increase to 1.17×10^{-5}mg.impact^{-1} and 1.29×10^{-5}mg.impact^{-1}. A sudden increase in rate losses occurs when occluding between 60-95%, 65-100% and 70-105%, where monomer loss rates were observed to be 2.41×10^{-5}mg.impact^{-1}, 2.06×10^{-5}mg.impact^{-1} and 2.24×10^{-5}mg.impact^{-1}. This increase in monomer loss rates around 100% occlusion could be attributed to solid-solid interface contact mechanisms, similar to earlier trends noticed during peristaltic pump studies.

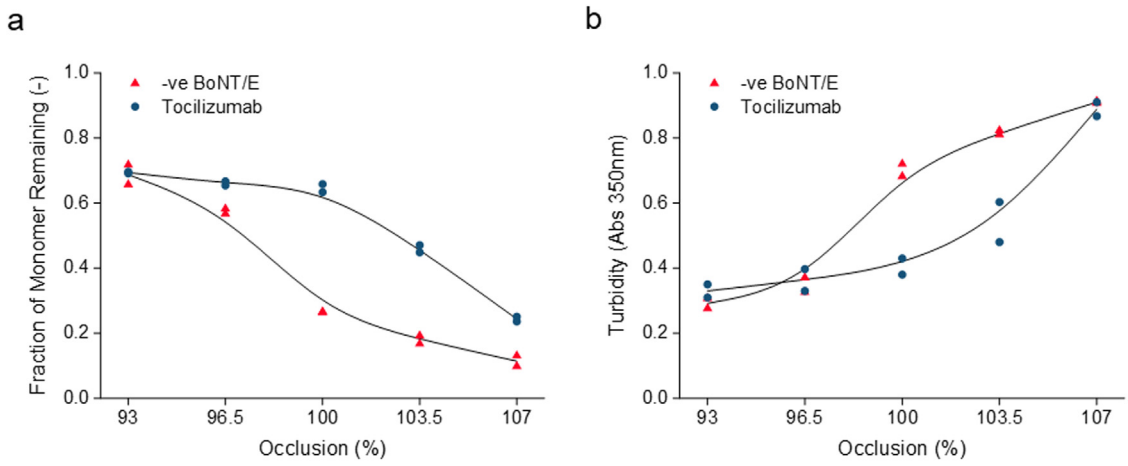

Figure 4. Interactions of the peristaltic rollers with the Masterflex® CFlex® L/S15 tubing and causing tocilizumab and –ve BoNT/E monomer loss are more evident as increasing compression and contact of solid-solid interfaces by changing occlusion further drive monomer loss and protein aggregate formation. **a** Different occlusion parameters were investigated at constant 80RPM during accelerated protein aggregation pumping studies using the closed-loop and two-model proteins, tocilizumab and –ve BoNT/E, both formulated at 0.4mg.ml^{-1} 100mM sodium phosphate 100mM sodium chloride (pH7.5). Fractions of monomer remaining after pumping studies are shown correlated against the occlusion parameter used. **b** Turbidity analysis of samples conducted at 350nm absorbance are correlated against the occlusion parameter selected during pumping.

Solid-Solid Interfacial Contact is a Function of Area and Rates of Monomer Loss in an Isolated Mechanism Method are Comparable to Peristaltic Pumping

Repeating the isolation study within the occlusion range 65-100% but using an occlusion block double the length of the previous, the amount of monomer remaining decreases from 90.3±0.7% to 85.3± 0.4% on duplicate average (Fig. 6c) – these monomer rates are reported as duplicate averages. The corresponding rate of monomer loss thus increased from 2.06 × 10^{-5}mg.impact^{-1} to 3.29 × 10^{-5}mg. impact^{-1} (Fig. 7c). Based on these rates, increasing the occluding block size by two-fold, and thus the contact area from 0.48cm^2. impact^{-1} to 0.96cm^2.impact^{-1}, corresponded with a rate change of 1.60-fold. Upon normalising them by the contact area per impact (cm^{-2}.impact^{-1}), these values area 4.30 × 10^{-5}mg.cm^{-2} and 3.43 × 10^{-5}mg.cm^{-2} (Fig. 7c). We normalised data to compare how much monomer is lost to solid-solid interface contact based on the respective contact areas during occlusion in peristaltic pumping and the solid-solid interface contact device.

We compared these rates to those obtained in our earlier accelerated protein aggregation studies using the peristaltic pump and closed-loop device. The contact area in a peristaltic pump can be

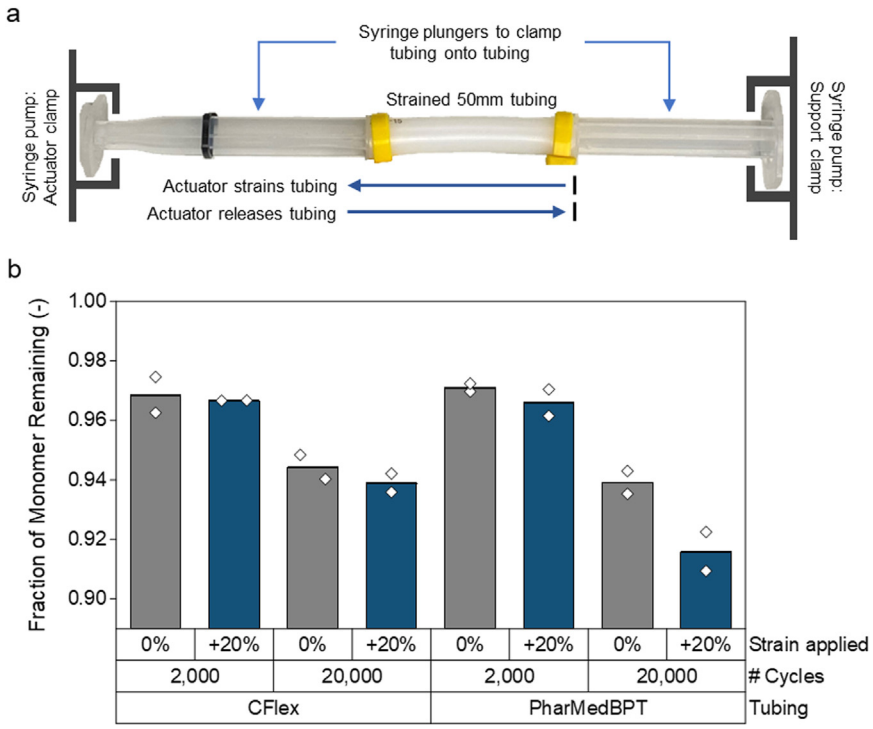

Figure 5. Controlled expansion-relaxation of Masterflex® CFlex® L/S15 tubing solid-liquid interfaces can lead to protein monomer loss and different tubing materials may affect this. **a** Illustration of the methodology used to show effect of expansion-relaxation of tubing pieces using a programmable syringe pump to apply strain. Tubing was filled with –ve BoNT/E formulated at 0.4mg.ml^{-1} 100mM sodium phosphate 100mM sodium chloride (pH7.5). **b** Fraction of remaining –ve BoNT/E monomer after conducting expansion-relaxation studies.

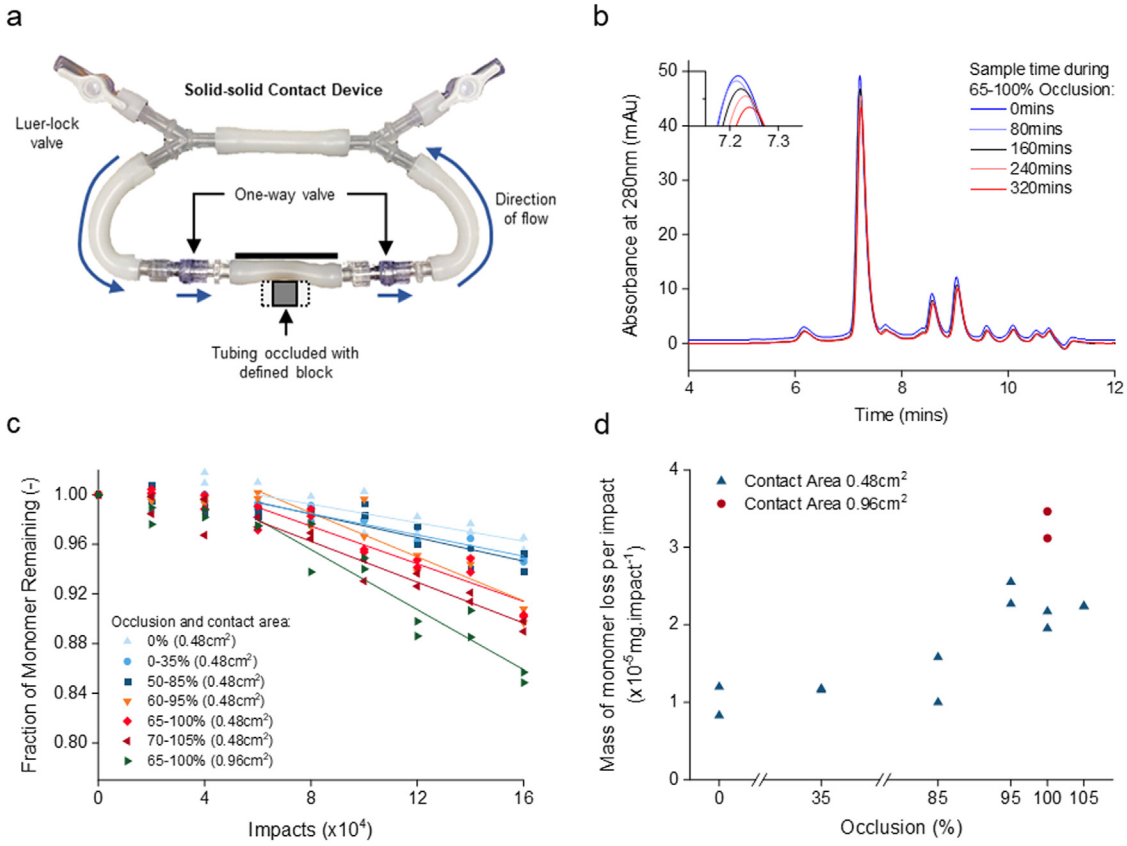

Figure 6. Isolation of solid-solid interface contact of peristaltic tubing inner walls was shown to cause protein monomer loss that is a function of the total interface area in contact. **a** Illustration of the solid-solid contact device used to isolated solid-solid interfacial contact of Masterflex® CFlex® L/S15 tubing via occlusion. **b** Size-exclusion ultra-performance chromatograms show analysis of samples which were removed from the device. Peaks of−ve BoNT/E monomer, eluting at 7.4mins, were integrated and the fraction of monomer remaining calculated for each time-based sample. **c** Fraction of remaining −ve BoNT/E monomer at different occlusion ranges are correlated against the number of impacts using the solid-solid contact device. Linear regressions shown are concatenate fits to duplicate data from the fourth-sample point with an average R^2 >0.81. **d** Rates of −ve BoNT/E monomer loss (x10^{-5}mg.impact^{-1}) obtained from the gradient of independent linear regressions of monomer loss data are correlated against occlusion.

modelled as a rectangle with length equal to the length of tubing that the roller is in contact with and a width equal to the tubing inner diameter – earlier, we measure this to be 4.8mm. The roller length was measured based on the outer surface of tubing that showed wearing from roller contact – we approximate this to be 30mm. Assuming that contact is made along the entirety of this distance, we calculate a contact area of 1.44cm^2.impact^{-1} (Fig. 7b). At 40RPM, the rate of monomer lost per impact was previously deemed to be 9.51×10^{-5}mg.impact^{-1}, based on four roller impacts per revolution, thus the corresponding rate or monomer loss normalised to area is 6.61×10^{-5}mg.cm^{-2} (Fig. 7c). 40RPM was chosen for comparison to limit heat effects and any spallation that may occur. A lower speed could not be chosen as the pump could not sustain regular compressions at slow speeds. Upon comparing the normalised rates based on contact area in isolated occlusion and pumping studies, the difference in monomer lost per area in these two different systems is within a 1.5- to 1.9-fold - the faster rates being for the peristaltic pump (Fig. 7c).

Discussion

Protein adsorption and aggregation is affected by temperatures.[28,29] During peristaltic pumping, a rotating pump head with rollers compresses elastic tubing to displace internal fluid. The rotation of rollers on tubing generates frictional heat whilst compressional forces create stored elastic potential energy that, upon release, also generates heat to cause protein aggregation. Deiringer et al investigated heat generation during peristaltic pumping operation using external thermal imaging to create a heat temperature profile inside the pump head.[8] In a different approach, we sought to internally measure and compare heat changes of the pumped solution and the surface of the inner tubing. We find that heat generation is strongly proportional to pump speed and the zone where tubing is compressed is the source of heat that dissipates into the pumped solution. Changing tubing type was also a strong factor, where switching from one tubing type to another doubled the heat gain.[28] When determining the effect of heat on monomer loss, providing cooling to the tubing to remove heat gain during pumping led to minor improvements in monomer recovery. The effect of heat maybe less of a concern when pumping larger volumes of solution during processing, such as in UF/DF, as it may have enough heat capacity to remove excess heat thus removing the need for refrigeration. The effect may be further lessened if the pumped protein has a higher T_m than the expected temperature build-up within the system. Although if temperature is a concern, process development should start with choosing the most suitable tubing and pump size to avoid excessive RPM. Otherwise, heat-induced aggregation during peristaltic pumping can be expected to be minimal.

Processes of protein adsorption and disruption-induced desorption can act synergistically to perpetuate protein aggregation.[30] Stages involved in this process include protein film establishment, protein film disruption and aggregate desorption to allow further protein film reconstitution. During protein film establishment, increasing time would allow more protein to contribute to this formation – this was observed as we manipulated pump speed. Whilst pumping, reducing pump speed from 160RPM to 40RPM increased time for adsorption in-between each roller impact 4.0-fold from

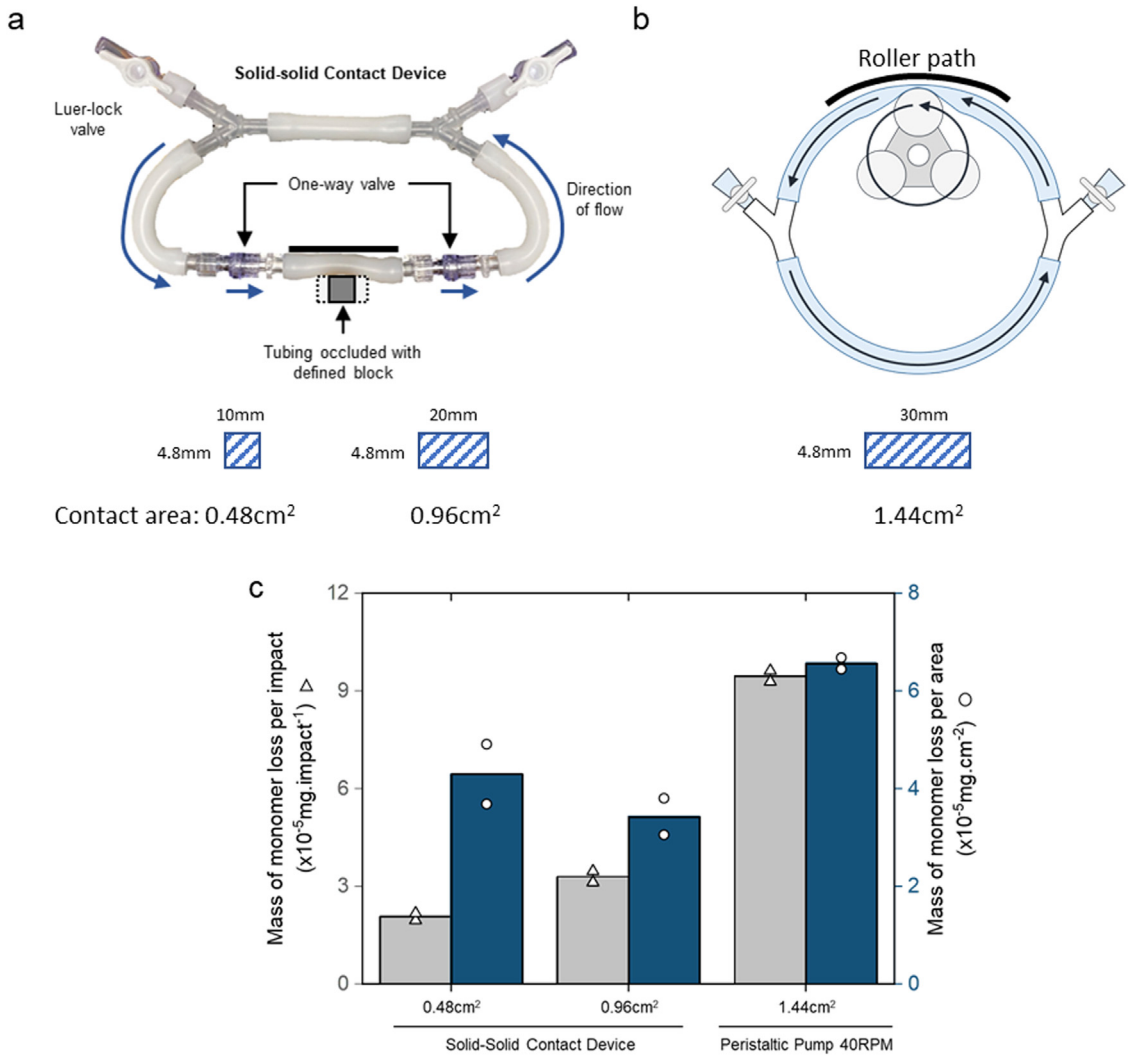

Figure 7. Comparison of the contact areas, over which contact of solid-solid interface contact occurs during different methodologies used, and the rates of monomer loss. **a** The contact area of the blocks used to occlude tubing during isolated solid-solid interface contact studies. **b** The contact area of the roller used in a peristaltic pump. **c** Comparison of monomer loss rates per impact subjected (x10^{-5}mg.impact^{-1}) (grey and triangle) and comparison of the rates of monomer loss per contact area (x10^{-5}mg.cm^{-2}) (blue and circle) achieved using the two-blocks, 0.48cm^2 and 0.96cm^2, in the isolated occlusion method and the peristaltic pump.

0.09s to 0.37s and led to an increase in monomer loss rates by ~2.0-fold. It has been reported that the time required for protein film constitution by adsorption is shorter than 1.0s (solid-liquid interface) – for air-liquid interfaces this can be less than 0.01s.[18,22] For solid-liquid interface adsorption, our pump adsorption times are within the reported time potentially making rates of monomer loss more susceptible to change upon pump speed. This process was also seen in the findings of Deiringer et al. and Wu et al. who showed this in the context of protein particle formation during peristaltic pump and piston pump operation.[8,31]

For efficient peristaltic pump operation, inner tubing walls should be in contact during roller compression to prevent internal back flow of liquid, called pump-slip, in high back pressure environments, such as in UF/DF, or when processing viscous fluids. Occlusion is the percentage of the total tubing wall thickness over the distance between the peristaltic roller compressing tubing and the peristaltic pump head wall where tubing is compressed against. During pumping in our studies, as tubing walls begin to contact at 100% occlusion, a sudden inflection of 20-35% of additional monomer loss was observed which suggested an additional mechanism compounding on the effects during under-occlusion (<100%) pumping. We attributed this effect to the disruption of protein films as inner tubing walls begin to contact each other upon each roller compression. Whilst this is important from a process yields perspective, it is important to understand that manipulating the compression of tubing may have secondary effects impacting aggregation that are discussed below.

Compression and flexing of tubing can deteriorate the inner tubing walls and leave deep cracks resulting in an increase in surface roughness.[32] When pumping, Greenblott et al. showed that older tubing, defined as the duration of time tubing is exposed to pumping, increased protein and foreign particle formation.[33] This effect is likely to be due to an increase in surface roughness due to the deterioration of tubing walls seen by Saunier and Yagoubi. Outside the context of peristaltic pumping, changing the surface roughness of rapidly spinning stainless steel discs, to generate high fluidic shear, led to changes in monomer loss.[34] As well as flexing causing cracks to appear, foreign particles of tubing may shed from tubing in a process called spallation – a problem long known in haemodialysis equipment.[35–37] Tube wall contacting frequency could exacerbate crack formation and increase spallation. We were aware of spallation and the increased formation of particles at the point of contact in our occlusion studies. Turbidity analysis would be able to detect these

particles in solution but in our work significant levels were not seen. Whilst we did not seek to investigate their effect further, other work has shown that the presence of foreign particles do not cause protein aggregation.[17,31] Thus, the increase of monomer loss which we show during pumping is primarily the result of contact of solid-solid interfaces that disrupt protein layers which form after protein adsorption

The fundamental interactions that peristaltic rollers have on tubing are complex but can be distilled down. Rotational and compressive forces on tubing may elicit monomer loss and protein aggregation through expansion-relaxation of tubing solid-liquid interfaces to shed protein films in a similar manner to those relaxation-dilation of air-liquid interfaces.[19,20] In addition, roller compressions can cause the contact of inner tubing solid-solid interfaces, which may also provide abrasive forces, to disrupt protein films in a similar manner to those during a rotating magnetic stirrer bar in contact with a beaker.[21] However, it is difficult to deconvolute the influence of these two mechanisms without the correct methodologies.

Consequently, we used a methodology like work published elsewhere[8] that involved repeatedly straining tubes containing protein solution to observe the effect of expansion-relaxation mechanisms in peristaltic tubing on monomer loss. When we strained tubing +20% for 20,000 times, we found evidence suggesting that this mechanism can contribute to monomer loss during peristaltic pumping, however tubing type appeared to affect the extent of loss where one tubing type made no difference in monomer loss compared to control tubes. The effect of tubing is also corroborated by the works of others where significant differences in subvisible protein particle concentrations were seen after straining different tubing types by 8.3% up to 2,000 times. We did not study which tubing materialistic properties caused this change, although it has been shown that a combination of tubing material composition and hardness influence protein particle formation.[25]

An understanding of the amount of tubing strain that occurs during peristaltic pumping is currently unknown. Deiringer et al. referenced Manopoulos et al. suggesting that a maximum of 30% of longitudinal stretching occurs in tubing during peristaltic pumping.[25,38] However, this value may instead quantify the deformation that is due to deep-occlusion of tubing at 130% (given the total tubing thickness of 2.0mm and the gap space of 1.4mm used in that model) and may only be true for the geometries of the model used for computational fluid dynamics (CFD) in that work.[38] Furthermore, when conducting CFD simulations of peristaltic pumping there is currently no CFD code that resolves fluid flow when occluding tubing at or above 100%.[38,39] As such as, the amount of tubing strain caused by roller compression and hydraulic power by fluid flow cannot be computed. However, it has been stated that rollers rotate about their own axis during tubing compression and reduce frictional forces.[39] This would reduce strain on the peristaltic tubing and expansion-relaxation of the tubing solid-liquid interface.

To isolate solid-solid interface contact from the rotational forces of the peristaltic roller, we developed a second isolation method. The device could control compressions on tubing to mimic occlusion whilst also being able to change the area of contact. When occluding tubing up to 85%, expansion-relaxation of tubing led to minimal changes in monomer loss compared to background losses that occurred during the control study at 0% occlusion (incubation). At 100% and 105% occlusion, the rate of monomer loss increased in a response like that seen when changing occlusion using the closed-loop device in the peristaltic pump. This occurred when solid-solid interfaces of tubing walls began to contact thus causing the mechanical disruption of protein films on tubing walls. At 95% occlusion, which implies that contact does not occur, the increase of monomer loss in line with 100% and 105% occlusion was not expected. As the gap space between inner tubing walls is 5% (0.2mm) of the internal tubing diameter at 95% occlusion, setup of the method may not be precise enough to make such fine changes and in this case inadvertently caused contact to occur. Finally, doubling the area over which solid-solid interface contact occurs at 100% occlusion showed that monomer loss via this mechanism is a function of contact area and led to 1.6-fold increase in rates of monomer loss.

We attempted to compare rates of monomer loss per contact area in the solid-solid contact method against those obtained during peristaltic pumping studies, however 1.5 to 1.9-fold differences in these rates were observed. Whilst these two methods subject tubing to occlusion, peristaltic pump rollers occlude tubing rotationally whilst our solid-solid contact method enacts linear occlusion. Rotational impact during occlusion in the pump could provide additional grinding or abrasion forces to the tubing surface during contact that disrupt protein films – these forces may be similar to those described previously.[21,23,24] We do not think that temperature or expansion-relaxation effects created by the rotational impacts contribute significantly to these differences, as our data suggests that these effects are minor.

During peristaltic pumping, we have now established that the solid-solid contact of inner tubing walls can lead to monomer loss and aggregation of therapeutic proteins. Our data suggests mechanical disruption of protein films on the tubing walls driven by the compression of the peristaltic pump rollers forcing contact to occur. As occlusion is a variable on peristaltic pumps, reducing this to allow a small gap between tubing walls to prevent solid-solid contact would reduce of monomer loss and additional effects such as spallation of tubing. However, reducing this too much could be counterproductive as it can risk lowering pumping efficiency resulting from fluid back slipping through partially occluded spaces existing between the inner tubing walls, particularly in high back pressure systems such as UF/DF. As adsorption and disruption of protein films are apparently synergistic, another approach to reducing monomer loss and aggregation would be using surfactants. Whilst their effect is not discussed in this study, it is known that correct addition of surfactants is synonymous with the decrease of monomer loss or protein particle formation.[3,6,8,21,31,34] Thus, preventing the establishment of a protein film on tubing interfaces will fundamentally limit the damage caused by tubing occlusion. However, adding surfactants is not always a suitable solution where their addition can be challenging to control upstream of UF/DF operations.[40] Finally, protein particles can form during pumping in final fill and finish[41] and whilst this work focuses on monomer loss quantification, due to the immunogenic risk that particles pose if they reach patients[12–14], the formation of particles during solid-solid contact of peristaltic tubing walls should be investigated. This can be further investigated with the help of novel machine learning techniques to better understand the particle morphologies that form because of these mechanisms.[33,42,43]

Conclusion

Several different mechanisms have been considered in this paper for their contribution in protein aggregation during peristaltic pumping. Heat generation was one such mechanism found to cause monomer loss although minor in proportion to losses by other mechanisms. When varying different process parameters, heat produced was proportional to the change in pump speed and originated from the frictional forces acted by the rollers on tubing, the properties of which can also cause changes in the heat produced. Pump speed had an inverse effect on the rate of monomer loss and reducing speed four-fold increased loss rates by 1.8- to 2.4-fold. This inverse effect could be the result of increased time allowed for protein adsorption and renewal of protein films, or the time that protein-protein interactions are allowed to occur upon tubing wall contact at slow pump speeds. Occlusion is a parameter that describes the amount of tubing compression. Varying this during pumping caused

an immediate 20-30% monomer loss upon the point tubing walls began to contact at 100% occlusion. Highlighting a significant change in the mechanisms at play and an allusion to abrasion or grinding of tubing interfaces upon their contact.

Occluding, or compressing, tubing during pumping can also cause strain to peristaltic tubing. Isolating this strain in continuous expansion-relaxation of the tubing interface in an isolated method outside of the pump caused minor monomer losses. This appears to not be a prominent mechanism that may occur during peristaltic pumping, although tubing material can affect the extent of monomer loss. In addition to strain, compression of tubing can drive the contact of peristaltic tubing inner walls. Isolating solid-solid interface contact in another isolated mechanism method led to monomer loss as a function of number of compressions and contact area. Comparing rates of monomer loss to pumping showed similarities, although higher losses in the pump is attributed to rotating rollers causing abrasion or grinding of interfaces during contact. This solid-solid contact mechanism is the likely primary mechanism of protein aggregation during peristaltic pumping, where contact disrupts protein films desorbing protein aggregates and allowing the reconstitution of protein films in a perpetuating cycle that is thus the peristatic pump's own Achille's heel.

Declaration of Competing Interest

The authors declare that they have no known competing financial interests or personal relationships that could have appeared to influence the work reported in this paper. C. Wilson and D. Gruber are employed by Ipsen Biopharm.

Acknowledgements

This work was supported by EPSRC Centre for Doctoral Training in Bioprocess Engineering Leadership (Complex Biological Products Manufacture) (EP/S021868/1) and Ipsen Biopharm Ltd. We appreciate the support from both Ipsen Biopharm and Ipsen Bioinnovation S. J.P in donating and preparing material for use in this work.

Supplementary Materials

Supplementary material associated with this article can be found in the online version at doi:10.1016/j.xphs.2023.08.012.

References

1. Wang S, Godfrey S, Ravikrishnan J, Lin H, Vogel J, Coffman J. Shear contributions to cell culture performance and product recovery in ATF and TFF perfusion systems. *J Biotechnol*. 2017;246:52–60. https://doi.org/10.1016/j.jbiotec.2017.01.020.
2. Nie J, Sun Y, Feng K, Huang L, Li Y, Bai Z. The efficient development of a novel recombinant adenovirus zoster vaccine perfusion production process. *Vaccine*. 2022;40(13):2036–2043. https://doi.org/10.1016/j.vaccine.2022.02.024.
3. Callahan DJ, Stanley B, Li Y. Control of protein particle formation during ultrafiltration/diafiltration through interfacial protection. *J Pharm Sci*. 2014;103(3):862–869. https://doi.org/10.1002/jps.23861.
4. Arunkumar A, Singh N, Schutsky EG, et al. Effect of channel-induced shear on biologics during ultrafiltration/diafiltration (UF/DF). *J Memb Sci*. 2016;514:671–683. https://doi.org/10.1016/j.memsci.2016.05.031.
5. Rosenberg E, Hepbildikler S, Kuhne W, Winter G. Ultrafiltration concentration of monoclonal antibody solutions: development of an optimized method minimizing aggregation. *J Memb Sci*. 2009;342(1-2):50–59. https://doi.org/10.1016/j.memsci.2009.06.028.
6. Her C, Tanenbaum LM, Bandi S, et al. Effects of tubing type, operating parameters, and surfactants on particle formation during peristaltic filling pump processing of a mAb formulation. *J Pharm Sci*. 2020;109(4):1439–1448. https://doi.org/10.1016/j.xphs.2020.01.009.
7. Her C, Carpenter JF. Effects of tubing type, formulation, and postpumping agitation on nanoparticle and microparticle formation in intravenous immunoglobulin solutions processed with a peristaltic filling pump. *J Pharm Sci*. 2020;109(1):739–749. https://doi.org/10.1016/j.xphs.2019.05.013.
8. Deiringer N, Friess W. Proteins on the rack: mechanistic studies on protein particle formation during peristaltic pumping. *J Pharm Sci*. 2022;111(5):1370–1378. https://doi.org/10.1016/j.xphs.2022.01.035.
9. Callahan DJ, Stanley B, Li Y. Control of protein particle formation during ultrafiltration/diafiltration through interfacial protection. *J Pharm Sci*. 2014;103(3):862–869. https://doi.org/10.1002/jps.23861.
10. Steinhauer T, Marx M, Bogendörfer K, Kulozik U. Membrane fouling during ultra- and microfiltration of whey and whey proteins at different environmental conditions: the role of aggregated whey proteins as fouling initiators. *J Memb Sci*. 2015;489:20–27. https://doi.org/10.1016/j.memsci.2015.04.002.
11. Jasulaityte G, Johansson HJ, Bracewell DG. Chromatography process development aided by a dye-based assay. *J Chem Technol Biotechnol*. 2020;95(1):132–141. https://doi.org/10.1002/jctb.6214.
12. Wang W, Singh SK, Li N, Toler MR, King KR, Nema S. Immunogenicity of protein aggregates - concerns and realities. *Int J Pharm*. 2012;431(1-2):1–11. https://doi.org/10.1016/j.ijpharm.2012.04.040.
13. Moussa EM, Panchal JP, Moorthy BS, et al. Immunogenicity of therapeutic protein aggregates. *J Pharm Sci*. 2016;105(2):417–430. https://doi.org/10.1016/j.xphs.2015.11.002.
14. Heljo P, Ahmadi M, Schack MMH, et al. Impact of stress on the immunogenic potential of adalimumab. *J Pharm Sci*. 2023;112:1000–1010. https://doi.org/10.1016/j.xphs.2022.12.027.
15. Simpson LW, Good TA, Leach JB. Protein folding and assembly in confined environments: implications for protein aggregation in hydrogels and tissues. *Biotechnol Adv*. 2020;42(June). https://doi.org/10.1016/j.biotechadv.2020.107573.
16. Dreckmann T, Boeuf J, Ludwig IS, Lümkemann J, Huwyler J. Low volume aseptic filling: impact of pump systems on shear stress. *Eur J Pharm Biopharm*. 2020;147:10–18. https://doi.org/10.1016/j.ejpb.2019.12.006. (December 2019).
17. Saller V, Hediger C, Matilainen J, et al. Influence of particle shedding from silicone tubing on antibody stability. *J Pharm Pharmacol*. 2018;70(5):675–685. https://doi.org/10.1111/jphp.12603.
18. Deiringer N, Rüdiger D, Luxbacher T, Zahler S, Frieß W. Catching Speedy Gonzales: driving forces for protein film formation on silicone rubber tubing during pumping. *J Pharm Sci*. 2022;111(6):1577–1586. https://doi.org/10.1016/j.xphs.2022.02.013.
19. Koepf E, Eisele S, Schroeder R, Brezesinski G, Friess W. Notorious but not understood: how liquid-air interfacial stress triggers protein aggregation. *Int J Pharm*. 2018;537(1-2):202–212. https://doi.org/10.1016/j.ijpharm.2017.12.043.
20. Bee JS, Schwartz DK, Trabelsi S, et al. Production of particles of therapeutic proteins at the air-water interface during compression/dilation cycles. *Soft Matter*. 2012;8(40):10329–10335. https://doi.org/10.1039/c2sm26184g.
21. Sediq AS, Van Duijvenvoorde RB, Jiskoot W, Nejadnik MR. No touching! Abrasion of adsorbed protein is the root cause of subvisible particle formation during stirring. *J Pharm Sci*. 2016;105(2):519–529. https://doi.org/10.1016/j.xphs.2015.10.003.
22. Žuntar T, Ličen M, Kuzman D, Osterman N. Real-time imaging of monoclonal antibody film reconstitution after mechanical stress at the air-liquid interface by Brewster angle microscopy. *Colloids Surf B Biointerfaces*. 2022;218(August):1–7. https://doi.org/10.1016/j.colsurfb.2022.112757.
23. Gikanga B, Eisner DR, Ovadia R, Day ES, Stauch OB, Maa YF. Processing impact on monoclonal antibody drug products: protein subvisible particulate formation induced by grinding stress. *PDA J Pharm Sci Technol*. 2017;71(3):172–188. https://doi.org/10.5731/pdajpst.2016.006726.
24. Jing ZY, Huo GL, Sun MF, Bin Shen B, Fang WJ. Characterization of grinding-induced subvisible particles and free radicals in a freeze-dried monoclonal antibody formulation. *Pharm Res*. 2022;39(2):399–410. https://doi.org/10.1007/s11095-022-03170-9.
25. Deiringer N, Friess W. Reaching the breaking point: Effect of tubing characteristics on protein particle formation during peristaltic pumping. *Int J Pharm*. 2022:627. https://doi.org/10.1016/j.ijpharm.2022.122216.
26. Zhou L, de Paiva A, Liu D, Aoki R, Dolly JO. Expression and purification of the light chain of botulinum neurotoxin A: a single mutation abolishes its cleavage of SNAP-25 and neurotoxicity after reconstitution with the heavy chain. *Biochemistry*. 1995;34(46):15175–15181. https://doi.org/10.1021/bi00046a025.
27. Fogolari F, Tosatto SCE, Muraro L, Montecucco C. Electric dipole reorientation in the interaction of botulinum neurotoxins with neuronal membranes. *FEBS Lett*. 2009;583(14):2321–2325. https://doi.org/10.1016/j.febslet.2009.06.046.
28. Kiesel I, Paulus M, Nase J, et al. Temperature-driven adsorption and desorption of proteins at solid–liquid interfaces. *Langmuir*. 2014;30(8):2077–2083. https://doi.org/10.1021/la404884a.
29. Jackman JA, Ferhan AR, Yoon BK, Park JH, Zhdanov VP, Cho N joon. Indirect nanoplasmonic sensing platform for monitoring temperature-dependent protein adsorption. Published online 2017. doi:10.1021/acs.analchem.7b03921.
30. Bee JS, Stevenson JL, Mehta B, et al. Response of a concentrated monoclonal antibody formulation to high shear. *Biotechnol Bioeng*. 2009;103(5):936–943. https://doi.org/10.1002/bit.22336.
31. Wu H, Randolph TW. Aggregation and particle formation during pumping of an antibody formulation are controlled by electrostatic interactions between pump surfaces and protein molecules. *J Pharm Sci*. 2020;109(4):1473–1482. https://doi.org/10.1016/j.xphs.2020.01.023.
32. Saunier J, Yagoubi N. Investigating the static or dynamic flexural and compressive stresses on flexible tubing: Comparison of clamp and peristaltic pump impact on surface damages and particles leaching during infusion acts. *J Mech Behav Biomed Mater*. 2021;123(May): 104737. https://doi.org/10.1016/j.jmbbm.2021.104737.
33. Greenblott DN, Zhang J, Calderon CP, Randolph TW. Machine learning approaches to root cause analysis, characterization, and monitoring of subvisible particles in

monoclonal antibody formulations. *Biotechnol Bioeng*. 2022. https://doi.org/10.1002/bit.28239. Published online.
34. Biddlecombe JG, Smith G, Uddin S, et al. Factors influencing antibody stability at solid-liquid interfaces in a high shear environment. *Biotechnol Prog*. 2009;25(5):1499–1507. https://doi.org/10.1002/btpr.211.
35. Bommer J, Pernicka E, Kessler J, Ritz E. Reduction of silicone particle release during haemodialysis. *Proc Eur Dial Transplant Assoc Eur Ren Assoc*. 1985;21:287–290.
36. Briceño JC, Runge TM. Tubing spallation in extracorporeal circuits. An in vitro study using an electronic particle counter. *Int J Artif Organs*. 1992;15(4):222–228.
37. Barron D, Harbottle S, Hoenich NA, Morley AR, Appleton D, McCabe JF. Particle spallation induced by blood pumps in hemodialysis tubing sets. *Artif Organs*. 1986;10(3):226–235. https://doi.org/10.1111/j.1525-1594.1986.tb02551.x.
38. Manopoulos C, Savva G, Tsoukalis A, et al. Optimal design in roller pump system applications for linear infusion. *Computation*. 2020;8(2). https://doi.org/10.3390/COMPUTATION8020035.
39. Manopoulos C, Tsoukalis A, Mathioulakis D. Suppression of flow pulsations and energy consumption of a drug delivery roller pump based on a novel tube design. *Proc Inst Mech Eng C J Mech Eng Sci*. 2022;236(14):7759–7770. https://doi.org/10.1177/09544062221084188.
40. Rafferty K, Ogunyankin MO, Ying W, Deshmukh S, Burton L, Chakravarthi S. Polysorbate 80 disposition following tangential flow filtration. *AIChE Annual Meeting*. 2017.
41. Nayak A, Colandene J, Bradford V, Perkins M. Characterization of subvisible particle formation during the filling pump operation of a monoclonal antibody solution. *J Pharm Sci*. 2011;100(10):4198–4204. https://doi.org/10.1002/jps.22676.
42. Witeof AE, Daniels AL, Rea LT, et al. Machine learning and accelerated stress approaches to differentiate potential causes of aggregation in polyclonal antibody formulations during shipping. *J Pharm Sci*. 2021;110(7):2743–2752. https://doi.org/10.1016/j.xphs.2021.02.029.
43. Thite NG, Ghazvini S, Wallace N, Feldman N, Calderon CP, Randolph TW. Machine learning analysis provides insight into mechanisms of protein particle formation inside containers during mechanical agitation. *J Pharm Sci*. 2022;111(10):2730–2744. https://doi.org/10.1016/j.xphs.2022.06.017.